Petroleum Science (2020) 17:1764–1778
https://doi.org/10.1007/s12182-020-00508-z

ORIGINAL PAPER

Distribution of nitrogen and oxygen compounds in shale oil distillates and their catalytic cracking performance

Xiao-Bo Chen[1] · Xin-Yang Zhang[1] · Ru-Meng Qin[1] · Sheng-Jie Shan[1] · Pan-Deng Xia[2] · Nan Li[1] · Jun Pu[1] · Ji-Xia Liu[1] · Yi-Bin Liu[1] · Chao-He Yang[1]

Received: 25 February 2020 / Published online: 15 September 2020

Abstract

The positive- and negative-ion electrospray ionization (ESI) coupled with Fourier transform-ion cyclotron resonance mass spectrometry (FT-ICR MS) was employed to identify the chemical composition of heteroatomic compounds in four distillates of Fushun shale oil, and their catalytic cracking performance was investigated. There are nine classes of basic nitrogen compounds (BNCs) and eleven classes of non-basic heteroatomic compounds (NBHCs) in the different distillates. The dominant BNCs are mainly basic N1 class species. The dominant NBHCs are mainly acidic O2 and O1 class species in the 300–350 °C, 350–400 °C, and 400–450 °C distillates, while the neutral N1, N1O1 and N2 compounds become relatively abundant in the > 450 °C fraction. The basic N1 compounds and acidic O1 and O2 compounds are separated into different distillates by the degree of alkylation (different carbon number) but not by aromaticity (different double-bond equivalent values). The basic N1O1 and N2 class species and neutral N1 and N2 class species are separated into different distillates by the degrees of both alkylation and aromaticity. After the catalytic cracking of Fushun shale oil, the classes of BNCs in the liquid products remain unchanged, while the classes and relative abundances of NBHCs vary significantly.

Keywords Molecular characterization · Shale oil · ESI FT-ICR MS · Nitrogen- and oxygen-containing compounds · Catalytic cracking performance

1 Introduction

Oil shale is generally defined as a fine-grained sedimentary rock containing an organic substance called kerogen. After the heat treatment of kerogen, it can be converted into liquid shale oil and combustible shale gas (Feng et al. 2013; Tong et al. 2011; Sun et al. 2014). Consequently, oil shale has received much attention worldwide due to its substantial reserves, and it is proposed to be a key alternative to conventional crude oil resources (Solum et al. 2014; Fletcher et al. 2014; Hillier et al. 2013). Shale oil and shale gas have already been the main energy resources in a few countries, and they have supplemented petroleum supplies in many countries throughout the world (Jin et al. 2012; Akash 2003; Hepbasli 2004). Shale oil is a complex organic mixture, and it contains thousands of hydrocarbons and heteroatomic organic compounds, such as sulfur-, nitrogen-, and oxygen-containing compounds (Tong et al. 2013; Chen et al. 2012). Shale oil can be refined into many useful products, such as transportation fuels and petrochemicals, in a manner similar to that of conventional crude oil (Yu et al. 2010). However, in comparison with some conventional crude oil, shale oil usually contains a relatively large content of nitrogen-, oxygen-, and/or sulfur-containing compounds. These heteroatomic compounds usually lead to processing problems, which affects the use of shale oil. For example, shale oil fuels become less stable over long periods of transport or storage; the catalysts used in the subsequent treatment are prone to poisoning; and corrosion and pollutant emission occur during their utilization (Chen et al. 2015; Yu et al. 2010). Consequently, many upgrading processes (e.g., acid neutralization, complexation, solvent extraction, and hydrotreatment) have been proposed to remove N, S, and

Edited by Xiu-Qiu Peng

✉ Xiao-Bo Chen
chenxiaobo@upc.edu.cn

[1] State Key Laboratory of Heavy Oil Processing, China University of Petroleum, Qingdao 266580, China

[2] Shandong Institute for Product Quality Inspection, Jinan 250102, China

O heteroatoms from shale oil (Chishti and Williams 1999; Williams and Chishti 2001). However, some heteroatomic compounds are also value-added chemicals or specialty chemicals, so shale oil can be potentially used as a feedstock to produce such chemicals (e.g., pyridine base and rust preventing oil) (Gao et al. 2019). Nevertheless, the lack of understanding of the chemical properties of heteroatomic compounds in shale oil and its distillates limits the future improvement of refining efficiency. Therefore, for better use of shale oil, it is significant to investigate the chemical composition and molecular structures of the heteroatomic species in shale oil and its distillates. In addition, identification of the heteroatomic compounds in shale oil at a molecular level is significant for geochemical research and for understanding the pyrolysis mechanism of kerogen as well (Stanford et al. 2006; Shi et al. 2010c).

In early decades, many studies have identified heteroatomic species in shale oils and their distillates by GC and/or GC–MS (Shue et al. 1981; Regtop et al. 1982; Korth et al. 1988). Nevertheless, the heteroatomic compounds need separation and concentration prior to analysis because they have low volatility and low concentrations in shale oils (Tong et al. 2013). More recently, Fourier transform-ion cyclotron resonance mass spectrometry (FT-ICR MS) has been widely applied to identify the heteroatomic compounds in fossil fuel samples. It is reported that FT-ICR MS coupled with laser desorption ionization (LDI), atmospheric pressure photoionization ionization (APPI), and electrospray ionization (ESI) can identify the heteroatomic compounds in shale oils at a molecular level (Jin et al. 2012; Cho et al. 2013; Bae et al. 2010). ESI can selectively ionize polar compounds in a dominant hydrocarbon matrix without the need of prior separation, such as basic and non-basic heteroatomic compounds under positive- and negative-ion modes, respectively. ESI coupled with FT-ICR MS can yield comprehensive classes (numbers of N, O, and S atoms in a molecule), types (numbers of rings plus double bonds), molecular weights, and alkylation (numbers of carbon atoms) distributions of the polar heteroatomic compounds (Stanford et al. 2006). Therefore, ESI FT-ICR MS has been widely employed to identify the nitrogen- and oxygen-containing species in crude oil and its distillates (Qian et al. 2001a; Klein et al. 2006; Shi et al. 2010a; Smith et al. 2008), coker gas oil (Zhu et al. 2011; Shi et al. 2010b), and shale oils (Jin et al. 2012; Tong et al. 2013; Chen et al. 2012; Bae et al. 2010).

In this paper, we identify the chemical composition and molecular structures of heteroatomic species in four distillates of Fushun shale oil, including their classes, types, and carbon numbers, by employing positive- and negative-ion ESI FT-ICR MS. As the distillation temperature increases, the chemical compositions and molecular structures of heteroatomic compounds will demonstrate the general trends of the Fushun shale oil composition. In addition, we investigate the catalytic cracking performance of different distillates derived from Fushun shale oil. The results of this paper will be helpful and essential in providing a more efficient and profitable process for refining shale oil into transportation fuels and specialty chemicals.

2 Experimental section

2.1 Analysis of the properties of Fushun shale oil and its distillates

Fushun shale oil employed in this work was supplied by the Fushun Mining Group, China. The oil was separated into five distillates by a true boiling point distillation unit according to the American Society for Testing and Materials (ASTM) D2892 and D5236 methods. The pressure was 2 mm of mercury when vacuum distillation was used. Additionally, the temperature of the liquid phase never exceeded 310 °C in all the distillation processes. The properties of Fushun shale oils are shown in Table 1 (the volatile fraction with a boiling point below 300 °C is not shown here). The Conradson carbon residue (CCR) was measured according to GB/T 268-87, which is a Chinese

Table 1 Properties of Fushun shale oil and its distillates

Sample	F_0	F_1	F_2	F_3	F_4
Distillation range, °C	Full range	300–350	350–400	400–450	> 450
Yield of fraction[a], wt%	100%	18.23	20.62	20.61	24.49
Density (20 °C), kg/m^3	894.3	868.4	885.9	896.3	974.9
CCR[b], wt%	1.55	0.06	0.16	0.32	6.37
C, wt%	85.08	84.33	85.04	85.17	85.42
H, wt%	12.04	12.53	12.39	12.31	11.53
H/C ratio	1.70	1.78	1.75	1.73	1.62
S, wt%	0.35	0.36	0.40	0.47	0.50
O[c], wt%	1.26	1.78	0.94	0.92	0.88
Total N (N_t), wt%	1.27	1.00	1.23	1.13	1.67
Basic N (N_b), wt%	0.63	0.61	0.63	0.60	0.90
N_b/N_t ratio, %	49.53	61.3	51.5	53.2	53.8
SARA analysis, wt%					
Saturates	49.64	67.24	62.46	59.96	33.60
Aromatics	16.70	13.08	15.64	15.86	22.08
Resins + asphaltenes	33.66	19.68	21.90	24.18	44.32

[a]The yield of the volatile fraction with a boiling point below 300 °C is 16.05 wt%

[b]CCR indicates the Conradson carbon residue

[c]The oxygen content is calculated by difference

standard analytical method for measuring carbon residue (Chen et al. 2012, 2015). The elemental contents of Fushun shale oil and its distillates were measured by employing a Vario EL III elemental analyzer (Elementar Co. Ltd., Germany). The group compositions (i.e., the content of saturates, aromatics, resins, and asphaltenes) were determined according to SY/T 5119-2008, which is a Chinese standard analytical method for determining the group compositions of heavy oil (Chen et al. 2012, 2015). The basic nitrogen content was measured using a perchloric acid–glacial acetic acid titration, and its detailed procedure can be found elsewhere (Han et al. 2013).

2.2 ESI FT-ICR MS analysis

Fushun shale oil and its distillates were dissolved in toluene at 10 mg/mL and further diluted with a toluene/methanol (3:7, v/v) solution at 20 mg/mL. For the negative-ion ESI mode, 15 μL of ammonium hydroxide was added to every 1 mL of prepared sample to enhance the ionization efficiency and reduce the suppression of ionic contaminants. For the positive-ion ESI mode, 5 μL of acetic acid was added to every 1 mL of prepared sample. All the solvents were analytically pure and distilled twice before use (Chen et al. 2012, 2014; Shi et al. 2010a, b, c).

The prepared samples were ionized by an Apollo II electrospray source and analyzed by a Bruker Apex-Ultra 9.4 T FT-ICR MS. For negative-ion mode, the spray shield voltage (SSV) was 3.5 kV, the capillary column front voltage (CFV) was 4.0 kV, and the capillary column end voltage (CEV) was − 320 V. Ions accumulated for 0.01 s in a hexapole under a direct-current voltage (DCV) of − 2.4 V and radio frequency (RF) amplitudes of 200 $V_{p\text{-}p}$. The ICR was operated at 13.5 db attenuation and from 100 to 1000 Da mass range. For positive-ion mode, the SSV was − 4.0 kV, CFV was − 4.5 kV, and CEV was 320 V. Ions accumulated for 0.001 in a hexapole with a DCV of 2.4 V and RF amplitudes of 200 V_{p-p}. The ICR was run at 13 db attenuation and from 100 to 1000 Da mass range. The *m/z* values were output to a spreadsheet when their relative abundance was larger than 6 times that of the standard deviation of the baseline noise value. The mass calibration and data analysis methods can be found in previous publications (Chen et al. 2012, 2014, 2017; Shi et al. 2010a, b, c).

In this paper, the chemical molecular formula of a given compound, $C_cH_hN_nO_oS_s$, was deduced in terms of the *m/z* values within ± 1 ppm. The double-bond equivalent (DBE) value of this compound, including the number of rings and double bonds, was calculated according to the equation of $DBE = c - h/2 + n/2 + 1$ (Chen et al. 2017).

2.3 Catalytic cracking performance tests

The catalytic cracking performance of Fushun shale oil and its distillates was investigated by employing a microactivity test (MAT) unit and a commercial equilibrium fluidized catalytic cracking (FCC) catalyst LVR-60R. The physicochemical properties of LVR-60R can be found elsewhere (Chen et al. 2016). Prior to each catalytic cracking test, the reactor was packed with 5 g of catalysts and purged at the reaction temperature for half an hour by a flow of N_2 at 30 mL/min. Next, the oil sample (approximately 1 g) was injected into the reactor at a uniform rate during 60 s, and then, the catalyst bed was stripped by a flow of N_2 at 30 mL/min for 10 min. The blowing gas from the reactor was cooled in ice water to obtain the gaseous and liquid products. A Bruker 456 gas chromatograph was employed to determine the composition of gaseous products, and subsequently the dry gas yield and liquefied petroleum gas (LPG) yield were obtained. The gasoline, light cycle oil (LCO), and heavy oil yields were obtained according to the simulated distillation (ASTM D2887) of liquid products determined by an Agilent 6890 N gas chromatograph. The cutoff points between the three liquid products were 205 °C and 350 °C. Moreover, the coke yield was determined according to the content of coke deposited on the stripped catalyst. For each catalytic cracking test, the weight hourly space velocity (WHSV) was controlled at 12 h^{-1}, the inlet flow rate of the oil sample was 1 g/60 s, the reaction temperature was 500 °C, and the ratio of catalyst to oil sample was 5. The total yield of all products is between 95% and 100%, which is relative to the feed injected for every run. The conversion of each distillate is calculated according to the sum of dry gas, LPG, gasoline, and coke yields (Chen et al. 2017; Xin et al. 2017).

3 Results and discussion

3.1 Properties of Fushun shale oil and its distillates

Table 1 shows that, for each distillate, its density and CCR value gradually increase, while its hydrogen content and H/C ratio gradually decrease with the increase in distillation temperature. These results are consistent with those of conventional crude oil distillates, while unlike conventional crude oil, the nitrogen content does not increase with the increase in fraction temperature (Snyder 1969; Shi et al. 2010c). The nitrogen content of F4 is the largest, followed by the nitrogen content of F2 and F3, and the nitrogen content of F1 is the smallest; however, the N_b/N_t ratio of F1 is the largest among all four distillates. These results indicate that some nitrogen compounds, especially basic nitrogen compounds, may be concentrated in a relatively narrow fraction range, not

uniformly distributed or regularly increasing or decreasing with the increase in fraction temperature.

3.2 Heteroatomic compounds characterization by positive-ion ESI FT-ICR MS

3.2.1 Mass distribution and relative abundance

Similar to conventional crude oil, the molecular weight (referring to the m/z value) and the number of basic nitrogen compounds (BNCs) in each distillate both gradually increase as the distillation temperature increases. The positive-ion ESI FT-ICR MS spectra of Fushun shale oil distillates are shown in Fig. 1. The F1 fraction exhibits 4220 peaks produced by various basic heteroatomic compounds, and these peaks show a nearly normal distribution between the mass distributions of $180 < m/z < 400$ with the number-average molecular weight (M_n) of 277. F2 exhibits 5672 peaks between the mass distributions of $200 < m/z < 460$ with the M_n of 312. F3 exhibits 6500 peaks between the mass distributions of $220 < m/z < 520$ with the M_n of 359. F4 exhibits 10,270 peaks between the mass distributions of $280 < m/z < 780$ with the M_n of 532. The number and molecular weight of BNCs increase with the increase in boiling point of fractions, which is similar to that of some conventional crude oils (Stanford et al. 2006; Shi et al. 2010c). Additionally, F4 contains some heteroatomic compounds with boiling points that are higher than 500 °C, and

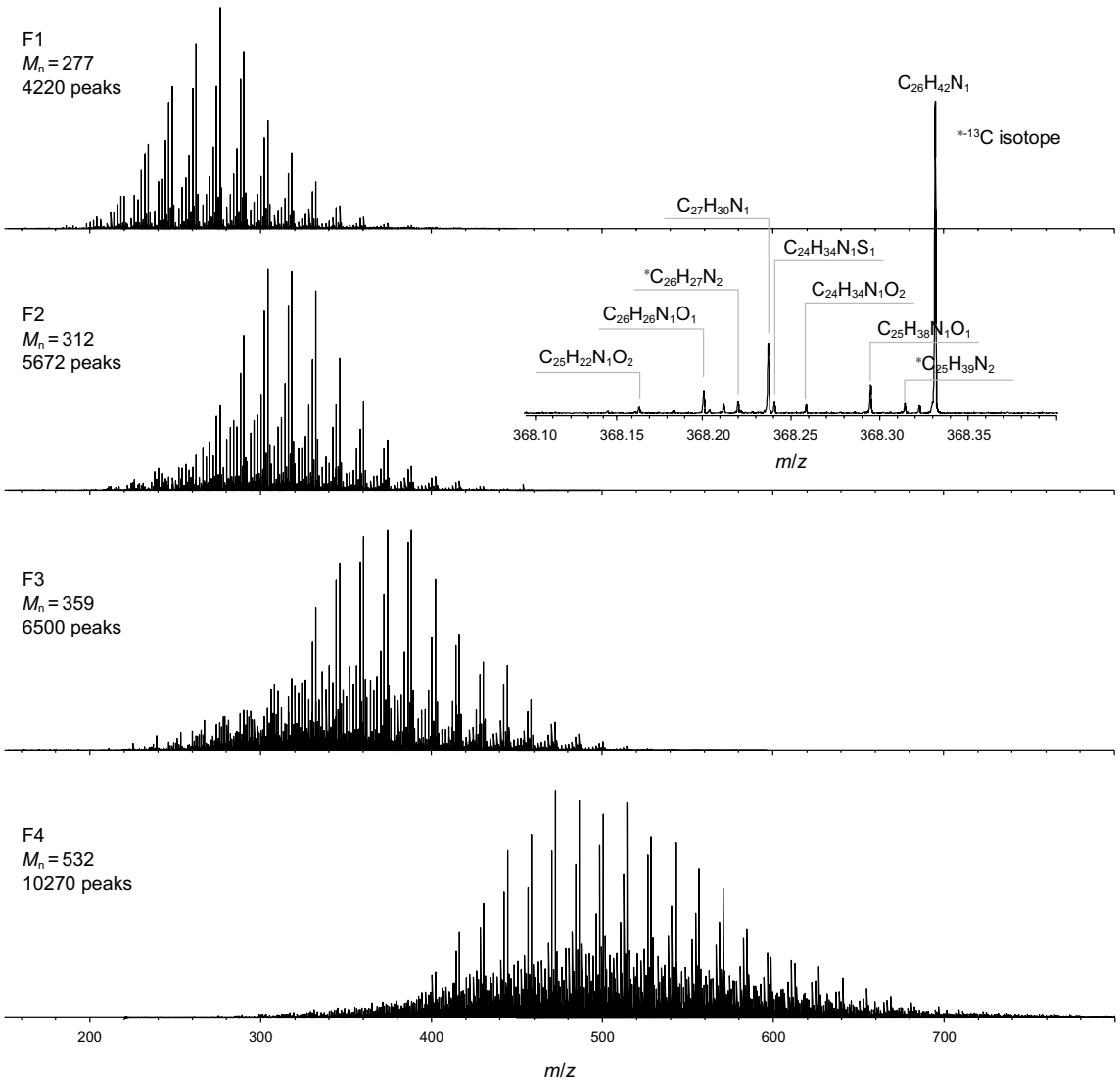

Fig. 1 Positive-ion ESI 9.4 T FT-ICR mass spectra of the Fushun shale oil distillates. Inserts show an example of the mass spectra magnification. Please refer to Table 1 for the meaning of F1–F4. M_n means the number-average molecular weight and its calculation method can be found elsewhere (Hughey et al. 2002b)

consequently, its mass range is much broader and the number-average molecular weight is much higher.

Figure 2 demonstrates that all the BNCs determined from the positive-ion ESI FT-ICR mass spectra can be divided into nine classes, namely, N1, N1O1, N1O2, N1O3, N2, N2O1, N2O2, N3, and N3O1. The classes of BNCs in the distillates are more abundant than those in their parent shale oil (Chen et al. 2012) and other shale oils [e.g., Green River shale oil (Bae et al. 2010), and Huadian shale oil (Tong et al. 2013)]. This result indicates that when shale oil is fractionated into narrow fractions, the concentration of some BNCs will increase due to uneven distribution in different fractions, and consequently, their relative abundances will increase. However, the classes of BNCs in Fushun shale oil are more abundant than that of conventional vacuum gas oil (VGO) derived from Annandale, New Jersey (Stanford et al. 2006). The latter has only six basic compound classes. This may have something to do with high levels of heteroatoms in shale oil. Through further analysis of Fig. 2, it is found that the species of BNCs in each fraction are not the same. For example, no N1O3 species are found in F4 fraction, no N3O1 species are found in F2 fraction, and no N1O3, N2O2, and N3O1 species are found in F3 fraction. These results directly demonstrate that some basic nitrogen compounds are concentrated in a relatively narrow fraction range, and moreover, the increase in spectral complexity and the number of mass spectra peaks as the distillation temperature increases is not simply due to more heteroatomic classes.

In addition, the relative abundance of the BNCs is remarkably different among each distillate (see Fig. 2). For example, the basic N1 compounds are always dominant in all the BNCs of each distillate; however, their relative abundance gradually decreases with the increase in distillation temperature. The relative abundance of N1 compounds in F1 (~86.13%) is much higher than that in F2 (~81.42%), F3 (~70.45%), and F4 (~47.16%). It is worth noting that relative abundance is completely different from absolute abundance. Even if the absolute abundance of a given compound is equal for two samples, its relative abundance may be different depending on the abundances of other compounds. However, for a given class of species, the general trend in abundance for different samples is clear. The relative abundances almost all increase with the increase in distillation temperature for the other BNCs that contain more than one heteroatom in their molecules, particularly for the N1O1 and N2 compounds. For instance, the relative abundances of the N1O1 and N2 compounds in the F1 fraction are only approximately 5%, while they can reach 11.23% and 25.89% in the F4 fraction, respectively. The results show that with the increase in boiling point of distillates, the number of multiatomic BNCs increases, which will make it more difficult to remove these heteroatoms from heavier shale oil distillates by hydrotreating processes (Chen et al. 2012). That is mainly because multiatomic compounds are more difficult to remove during hydrogenation than compounds containing only one heteroatom (Fu et al. 2006).

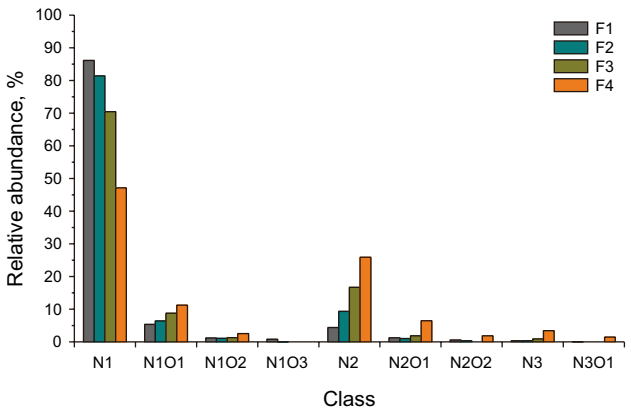

Fig. 2 Relative abundances (>0.5%) of the basic heteroatomic classes in the Fushun shale oil distillates. Please refer to Table 1 for the meaning of F1–F4

3.2.2 Molecular composition of BNCs

To further understand the distribution of the molecular structures of BNCs in the Fushun shale oil distillates, Fig. 3 shows the relative abundance plots of DBE versus carbon number (C_n) of the N1, N1O1, and N2 classes. Figure 4 demonstrates the suggested molecular structures of these compounds based on their DBE values.

As can be seen from Fig. 3a, with the increase in distillation temperature, the DBE values and carbon numbers of basic N1 species increase to some extent, especially for F4 fraction. However, in all fractions, the DBE value of basic N1 compounds does not change much, and N1 compounds with DBE of 4 and 5, corresponding to pyridines and tetrahydroquinolines (Fig. 4a and b shows their suggested core structures), always take the dominant position. It should be noted here that although the DBE value of anilines is also 4, our previous research shows that Fushun shale oil contains almost no aniline (Chen et al. 2012). With the increase in boiling point of distillates, the main change is their carbon number. For example, the pyridines and tetrahydroquinolines are mainly centered at C_n of 16–22 in F1, 19–26 in F2, 22–31 in F3, and 29–44 in F4. Thus, these basic N1 class species are mainly separated into different distillates by alkylation (different C_n) but not by aromaticity (different DBE values). The basic N1 compounds have the same aromatic core structures in different narrow fractions, while the length and quantity of the alkyl side chains are different. These results will help us to reveal the transformation pathway of basic N1 compounds in FCC and their poisoning effect on FCC catalysts easily (Chen et al. 2012, 2017). The

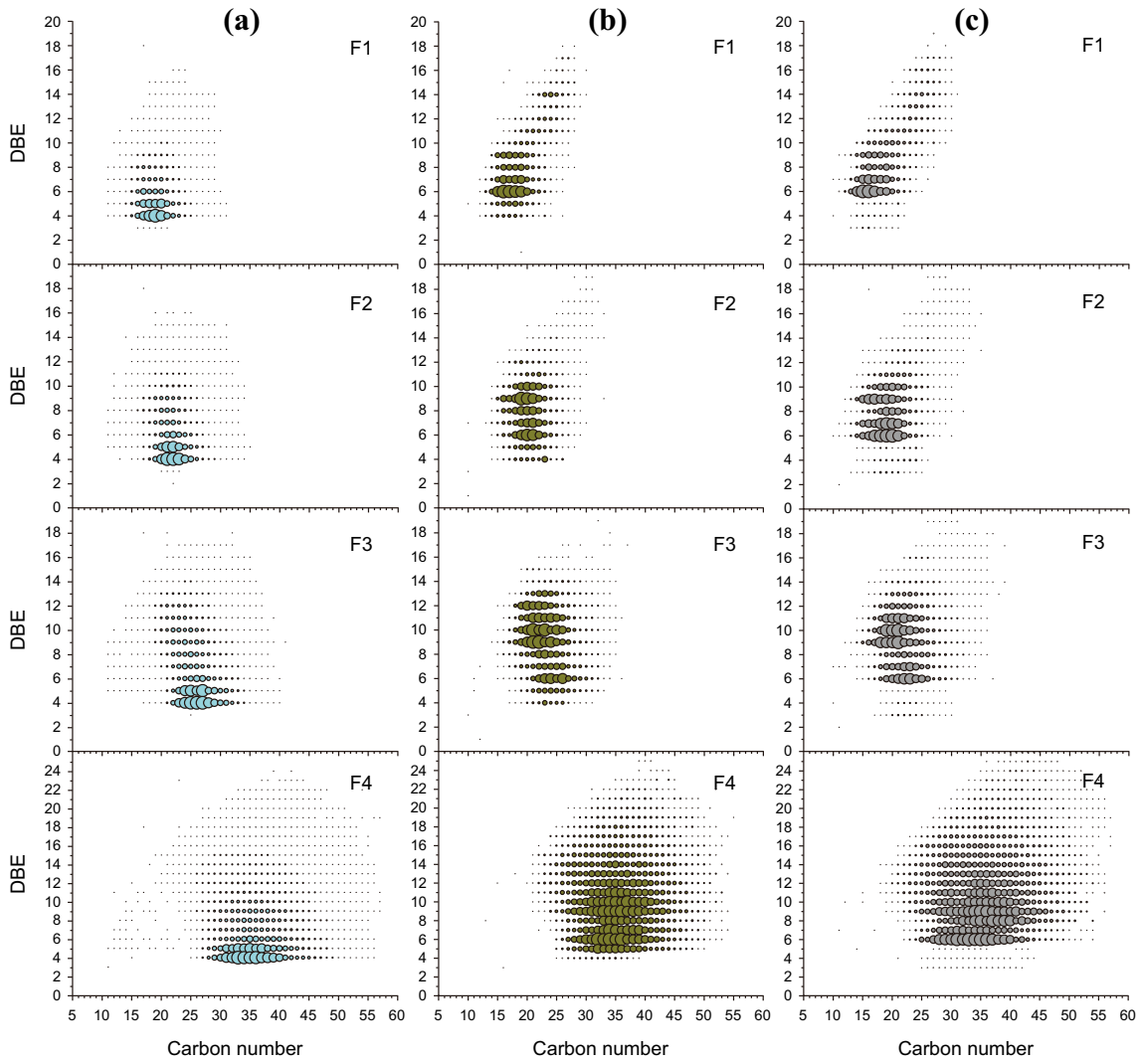

Fig. 3 Relative abundance plots of DBE versus carbon number of (**a**) N1, (**b**) N1O1, and (**c**) N2 basic compounds in the Fushun shale oil distillates. The area of a circle shows the relative abundance of each heteroatomic compound. Please refer to Table 1 for the meaning of F1–F4

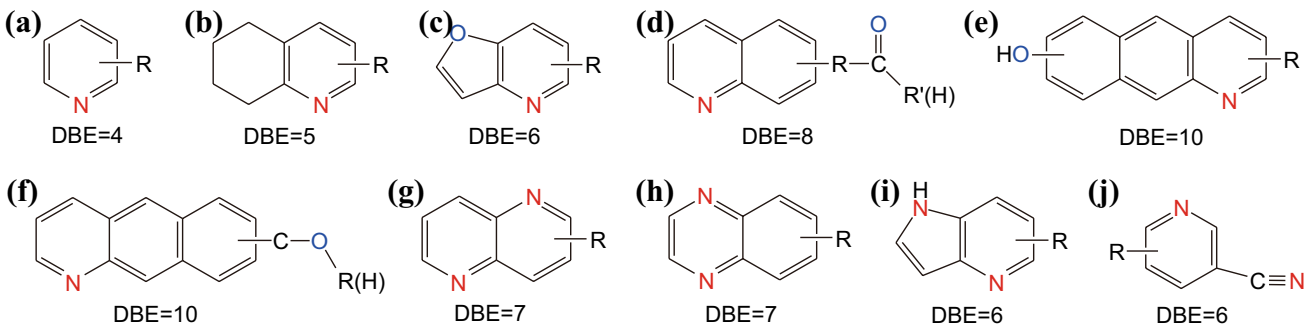

Fig. 4 Suggested structures of basic heteroatomic species in the Fushun shale oil distillates

basic N1 class species usually undergo side chain cracking first during the catalytic cracking process, and then, an almost identical aromatic structure remains finally (Chen et al. 2017; Li et al. 2011). Therefore, if we want to understand the deactivating effect of these basic N1 compounds on catalysts, we just need to determine the catalytic cracking pathways and deactivating mechanism of these heterocyclic core structures (e.g., pyridine ring and tetrahydroquinoline ring).

The DBE values and carbon numbers of basic N1O1 and N2 class species both gradually increase as the distillation temperature increases, particularly for F4 (see Fig. 3b and c). The basic N1O1 class species are mainly concentrated at DBE = 6, 7 and C_n = 15–20 in F1, while they are mainly concentrated at DBE = 6–10 and C_n = 18–22 in F2, DBE = 6, 9–12 and C_n = 19–26 in F3, and DBE = 5–15 and C_n = 28–43 in F4. The degrees of aromaticity and alkylation of the basic N1O1 class species in each distillate increase with the increase in distillation temperature. Moreover, the N1O1 class species with a given DBE value have a narrow carbon number range in each distillate (see Fig. 3b). Therefore, these species are separated into different distillates by the degrees of both alkylation and aromaticity, which is different from basic N1 class species. Previous publications report that oxygen exists mainly in the form of C–O–C (ether), C–OH (phenol and alcohol), and C=O (carbonyl) in the kerogen as determined by the XPS, FT-IR, and ^{13}C NMR analyses (Kelemen et al. 2007). Phenols, naphthols, furans, ketones, and ethers have been observed in shale oils by GC–MS (Shue and Yen 1981; Regtop et al. 1982; Korth et al. 1988). Consequently, the suggested core structures of basic N1O1 compounds in the Fushun shale oil samples are illustrated in Fig. 4 according to their DBE values and the structures reported previously. It is well known that an additional aromatic ring is fused to the aromatic core for every three additional DBE units. Therefore, some typical suggested core structures are listed in Fig. 4. In addition to a pyridine ring in their molecules, the oxygen functional groups are probably furans (Fig. 4c), ketones or aldehydes (Fig. 4d), phenols or naphthols (Fig. 4e), and ethers or alcohols (Fig. 4f). Although it is reported that the ESI efficiency of furans, aldehydes, and ketones is relatively low, the pyridine rings of the N1O1 compounds can be efficiently determined by positive-ion ESI FT-ICR MS (Stanford et al. 2006; Hughey et al. 2002a). Therefore, these compounds have an approximately 5–11% relative mass peak abundance in positive-ion mode (refer to Fig. 2).

As shown in Fig. 3c, the dominant basic N2 class species are mainly concentrated at DBE = 6, 7 and C_n = 14–20 in F1, DBE = 6–10 and C_n = 15–22 in F2, DBE = 6, 7, 9–11 and C_n = 16–26 in F3, and DBE = 6–14 and C_n = 25–46 in F4. Consequently, the N2 class species are also separated into different distillates by the degrees of both alkylation and aromaticity. Concerning the molecular core structure of the N2 class species, they probably contain two pyridine rings (Fig. 4g) or one ring containing two nitrogen atoms (Fig. 4h). These species also probably contain pyridine and pyrrole rings in one molecule (Fig. 4i) at the same time, and now the N2 compounds are amphoteric molecules (Smith et al. 2008; Han et al. 2013). These species can also contain a pyridine ring and a nitrile group (Fig. 4j), namely, aromatic nitriles, which have been identified in the Fushun shale oil samples by GC–MS analysis (Shue and Yen 1981).

3.3 Heteroatomic compounds characterization by negative-ion ESI FT-ICR MS

3.3.1 Mass distribution and relative abundance

Figure 5 demonstrates that the peaks of non-basic heteroatomic compounds (NBHCs) do not exhibit normal distributions similar to those of the BNCs within the mass range of each distillate. F1 contains various non-basic heteroatomic compounds with 1862 peaks between the mass distributions of $180 < m/z < 420$ with M_n of 292. F2 exhibits 2893 peaks between the mass distributions of $200 < m/z < 440$ with M_n of 327; F3 exhibits 3284 peaks between the mass distributions of $220 < m/z < 480$ with M_n of 362; and F4 exhibits 3937 peaks between the mass distributions of $220 < m/z < 580$ with M_n of 391. Similar to the results of BNCs, the m/z value, the spectral complexity, and the number of BNHCs in each distillate increase as the distillation temperature increase. However, the number of peaks of NBHCs is much lower than that of the BNCs in each distillate. This result can be explained by the lower ionization efficiency of the non-basic heteroatomic compounds determined by negative-ion ESI. These results are similar to analysis results of VGO derived from Annandale, NJ crude oil. Basic compounds are more varied than non-basic components: 720 and 1183 non-basic species resolved in the middle and heavy VGO distillates, compared to 2404 and 2875 basic species in the middle and heavy VGO distillates (Stanford et al. 2006).

Figure 6 demonstrates that there are eleven classes of NBHCs in Fushun shale oil distillates, namely, N1, N2, N1O1, N2O1, N1O2, N2O2, N1O3, O1, O2, O3, and O4. Similar to the BNCs, the classes of NBHCs in the Fushun shale oil distillates are also more abundant than those in their parent shale oil (Chen et al. 2012), Green River shale oil (Bae et al. 2010) and Huadian shale oil (Tong et al. 2013). They also more abundant than those in crude oil from Annandale, NJ and Bohai basin, China (Stanford et al. 2006; Shi et al. 2010c). By further analyzing Fig. 6, the relative abundance of NBHCs is remarkably different in each distillate. The dominant compounds of F1 are acidic O2 compounds with a relative abundance of 29.96%, followed by O1 compounds with a relative

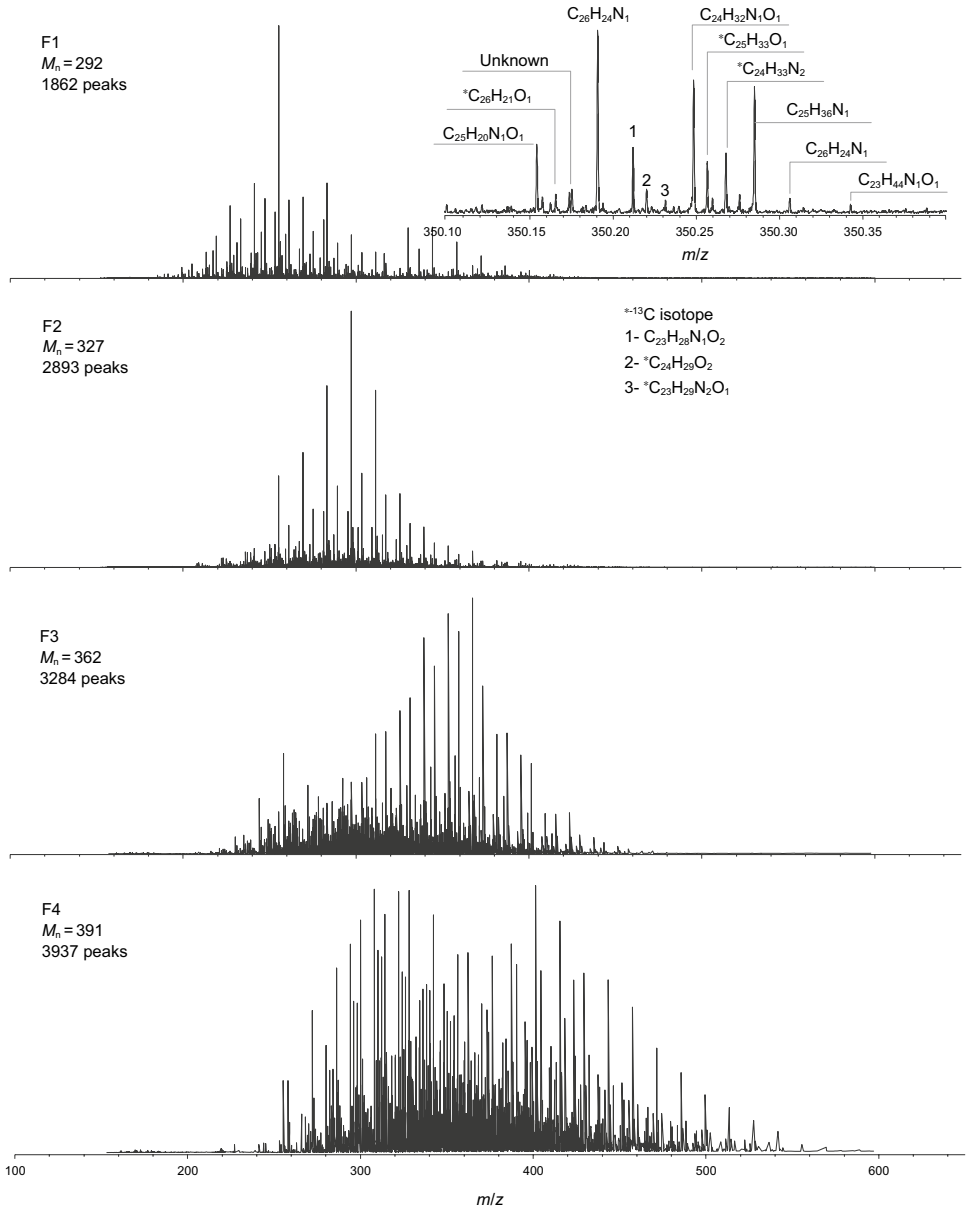

Fig. 5 Negative-ion ESI 9.4 T FT-ICR mass spectra of Fushun shale oil distillates. Inserts show an example of the mass spectra magnification. Please refer to Table 1 for the meaning of F1–F4

abundance of 23.33%. Concerning F2, the dominant species are also O2 and O1 compounds with relative abundances of 35.52% and 24.06%, respectively. In F3, the relative abundance of O1 compounds is slightly larger than that of O2 compounds; the relative abundances of these compounds are 25.40% and 24.25%, respectively. However, for F4, the dominant species were neutral N1 class species (29.81%), followed by O1 class species (15.94%). In the F1, F2, and F3 distillates, the abundant NBHCs are mainly acidic oxygen compounds, such as O2 and O1 compounds, while the neutral nitrogen compounds, such as N1, N1O1, and N2 compounds, become relatively abundant in the F4 distillate. The O4 class species is observed exclusively in F1 and F2. These results further illustrate that some heteroatomic compounds may accumulate in some relatively narrow distillates. This also indicates some NBHCs (e.g., NiO3 and O4) have poor stability, causing them to disappear in high boiling fractions. In addition, the difference in the relative abundance between two given classes of NBHCs (e.g., N1 and N1O1 class species) in each distillate is much smaller compared with that of the BNCs. As mentioned before, the basic N1 compounds are predominant in all BNCs.

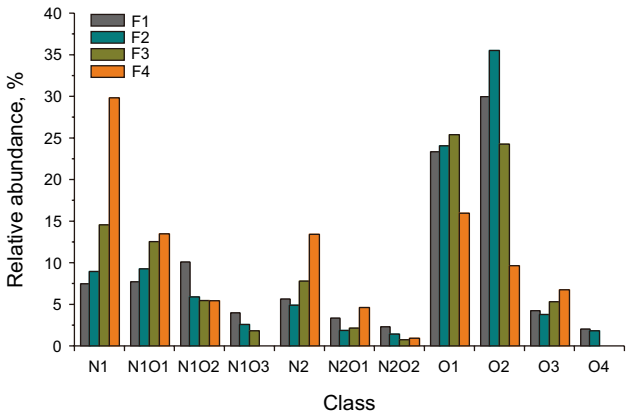

Fig. 6 Relative abundances (> 0.5%) of non-basic heteroatomic compounds in the Fushun shale oil distillates. Please refer to Table 1 for the meaning of F1–F4

3.3.2 Molecular composition of NBHCs

To further understand the distribution of the NBHCs molecular structure in the Fushun shale oil distillates, the relative abundance plots of DBE versus carbon number of non-basic N1, N1O1, and N1O2 compounds are demonstrated in Fig. 7. The suggested structures of these compounds according to their DBE values and the structures reported previously are illustrated in Fig. 8. Moreover, the relative abundance plots of DBE versus carbon number of non-basic N2, O1, and O2 compounds are demonstrated in Fig. 9.

As shown in Fig. 7a, the dominant neutral N1 class species are mainly concentrated at DBE = 6 and C_n = 15–21 in F1, while they are mainly concentrated at DBE = 6, 9 and C_n = 16–23 in F2, at DBE = 6, 9, 12 and C_n = 18–27 in F3, and at DBE = 9, 12, 15 and C_n = 20–31 in F4. The DBE values of the dominant neutral N1 compounds increase, and

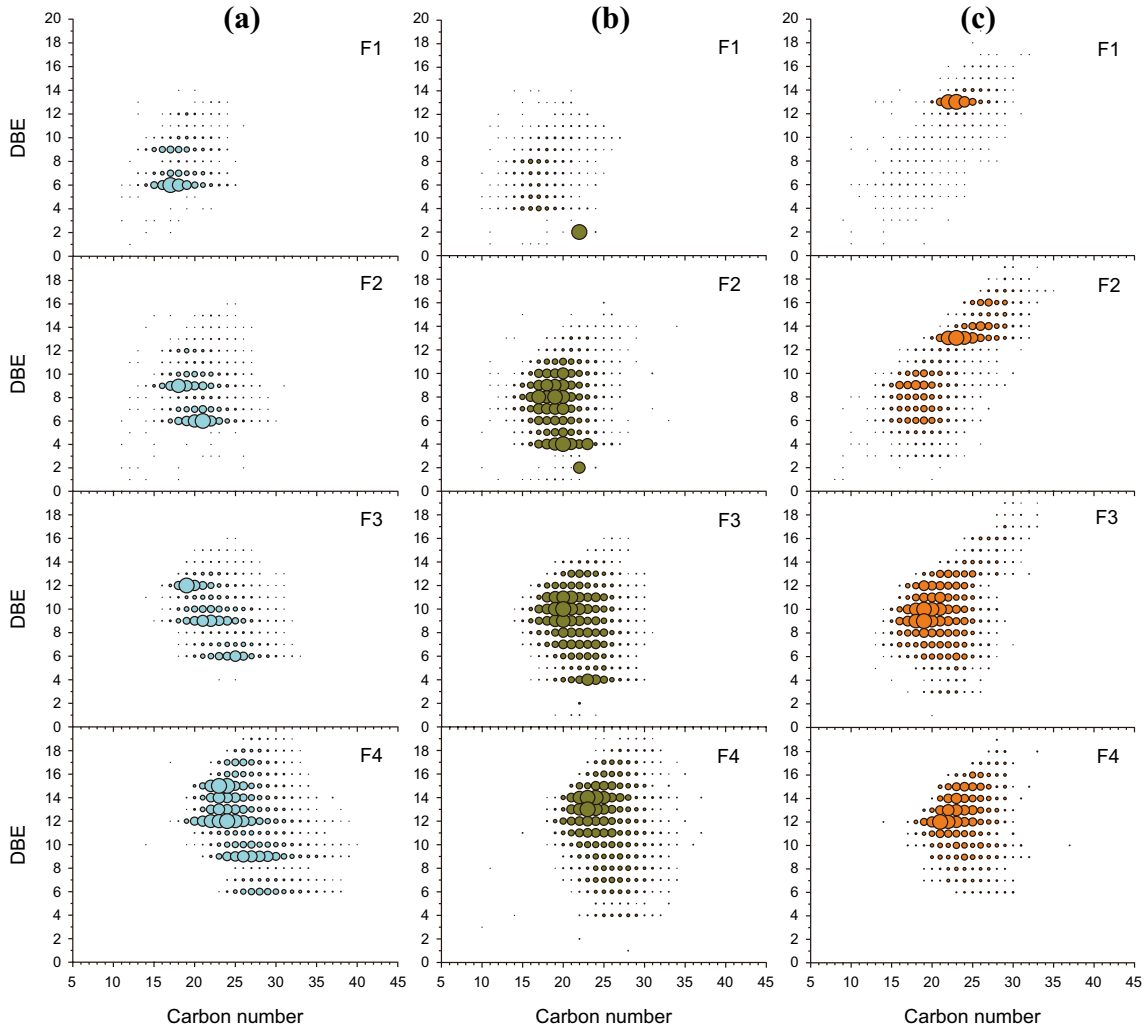

Fig. 7 Relative abundance plots of DBE versus carbon number of the neutral (**a**) N1, (**b**) N1O1, and (**c**) N1O2 compounds in the Fushun shale oil distillates. The area of a circle shows the relative abundance of each heteroatomic compound. Please refer to Table 1 for the meaning of F1–F4

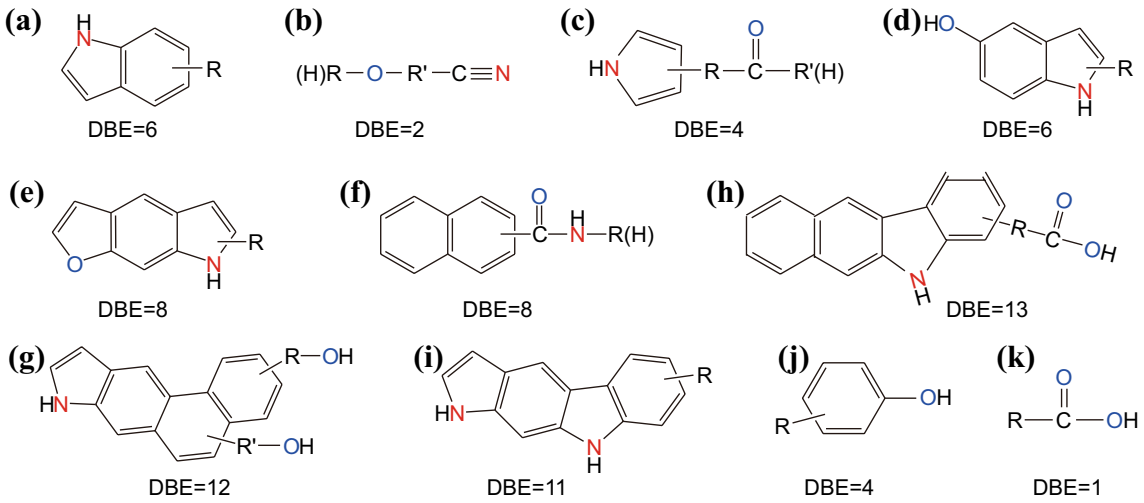

Fig. 8 Suggested structures of the non-basic heteroatomic compounds in the Fushun shale oil distillates

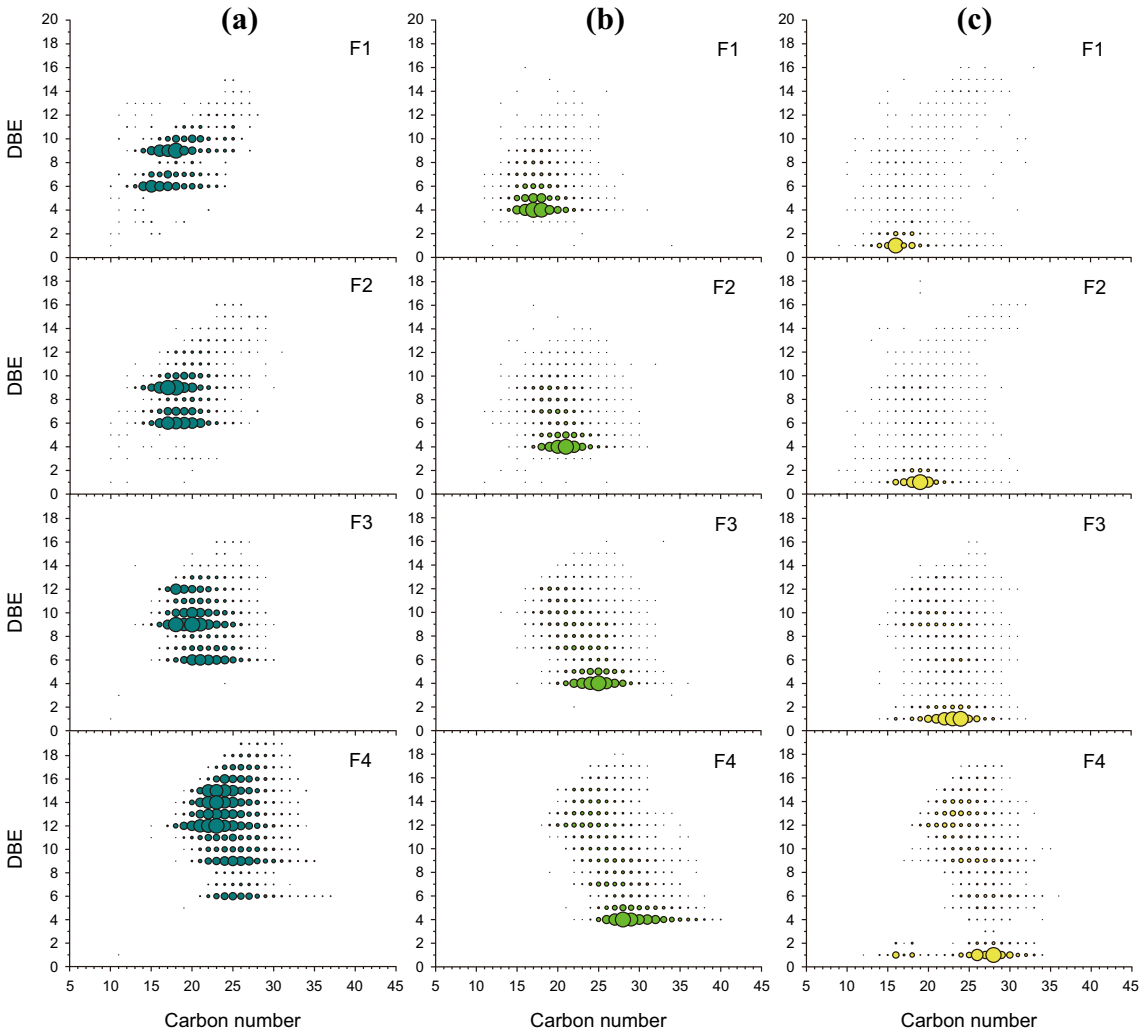

Fig. 9 Relative abundance plots of DBE versus carbon number of non-basic (**a**) N2, (**b**) O1, and (**c**) O2 compounds in the Fushun shale oil distillates. The area of a circle shows the relative abundance of each heteroatomic compound. Please refer to Table 1 for the meaning of F1–F4

the carbon number has a slight increase and a slight overlap as the distillation temperature increases. Thus, these compounds are mainly separated into different distillates by the degree of aromaticity, with the degree of alkylation as a supplement. These dominant neutral N1 compounds are presumably indoles (referred to Fig. 8a), carbazoles, and benzocarbazoles, which is consistent with the results of their parent shale oil, Huadian shale oil and crude oil from Bohai basin, China (Chen et al. 2012; Tong et al. 2013; Shi et al. 2010c).

The dominant neutral N1O1 compound in F1 is specie with value of DBE = 2 and C_n = 22 (refer to Fig. 7b), which are probably aliphatic nitrile containing hydroxyl groups (Fig. 8b). However, it should be contaminant because no continuous distribution in abundance of its homologues, although these aliphatic nitriles have been observed in Fushun shale oil by GC–MS analysis as reported in a previous publication (Guo et al. 1993). For the other distillates, the dominant neutral N1O1 class species are mainly concentrated at DBE = 2, 4–10 and C_n = 16–23 in F2, at DBE = 4, 7–11 and C_n = 17–25 in F3, and at DBE = 11–15 and C_n = 20–28 in F4. Concerning the N1O1 class species, in addition to a pyrrole ring in their molecules, the oxygen functional groups are probably carbonyl (Fig. 8c), hydroxyl (Fig. 8d), and furans (Fig. 8e). Moreover, these species are likely amides (Fig. 8f), which have been widely determined to exist in shale oil by GC–MS analysis (Shue et al. 1981; Regtop et al. 1982; Korth et al. 1988). Figure 7c shows that the dominant N1O2 compounds in the Fushun shale oil distillates are at DBE = 9, 10, 12, and 13, and their probable core structures are demonstrated in Fig. 8g and Fig. 8h. In addition, a pyrrole ring, these compounds may contain two hydroxyl or carboxyl groups in their molecules.

The neutral N2 compounds have a similar distribution of DBE values and carbon number compared to the neutral N1 compounds (compare Fig. 7a with Fig. 9a). The N2 compounds are concentrated at DBE = 6, 9, and 12–15 and are mainly separated by the degree of aromaticity into different distillates. These compounds probably contain two pyrrole rings and their suggested structures are listed in Fig. 8i. In addition, these compounds also probably contain a pyridine and a pyrrole ring in one molecule at the same time and now the N2 compounds are amphoteric molecules (Smith et al. 2008; Han et al. 2013), like the basic N2 class species (refer to Fig. 4i).

According to previous reports, the common O1 compounds are phenols, aldehydes, furans and ketones in conventional crude oil (Stanford et al. 2006). However, except for phenols that can selectively undergo ionization by ESI, aldehydes, furans, and ketones present much less efficient ionization in the negative-ion ESI mode (Hughey et al. 2002a). As seen from Fig. 9b, the dominant non-basic O1 class species are always concentrated at DBE = 4 in each distillate, while their carbon number gradually increases as the distillation temperature increases. Thus, these O1 class species are separated into different distillates by alkylation but not by aromaticity, which is consistent with the basic N1 class species. These species are likely phenols (Fig. 8j), which are present in a relatively higher concentration and have been determined widely in some shale oils by GC–MS analysis (Shue et al. 1981; Regtop et al. 1982; Korth et al. 1988). Snyder (1969) reported phenols exhibiting in heavy distillates (850-1000 °F) of Californian crude oil with 4 < DBE < 11, with the most abundant at DBE = 5. The analysis of the distribution of aromatic mono-oxygen species from the VGO of an Annandale crude oil shown that phenols exhibited DBE values that ≥ 4 (Stanford et al. 2006). Here, phenols in different distillates of Fushun shale oil also shown DBE values that ≥ 4, while the difference is that the most abundant is DBE = 4. The concentration of these phenolic compounds in Fushun shale oil is relatively high, and consequently, after enrichment and separation, they have the potential to be used as the raw materials for the production of colophonies, fungicides, and preservatives (Gao et al. 2019).

Another kind of oxygen compound is the acidic O2 class species. As shown in Fig. 9c, the O2 compounds in each distillate are always concentrated at DBE = 1. Similar to the O1 class species, these compounds are mainly separated into different distillates by alkylation but not by aromaticity. These compounds are aliphatic acids (Fig. 8k). The dominant acidic O2 class species are C_{16} aliphatic acids in F1, and the dominant acidic O2 class species are $C_{17–30}$ aliphatic acids in the other three heavier distillates. It must be stated here that these C_{16} aliphatic acids may also be the contaminants brought during the analysis. Interestingly, the relative abundance of naphthenic acids (DBE > 1) is exceedingly small in all distillates. This result is not consistent with some conventional crude oil (e.g., the crude oil from Annandale NJ and Bohai basin, China), in which most O2 compounds may be aromatic carboxylic acids and/or polycyclic naphthenic acids (Stanford et al. 2006; Kelemen et al. 2007; Jones et al. 2001; Qian et al. 2001b).

3.4 Catalytic cracking performance of Fushun shale oil and its distillates

The catalytic cracking performance of Fushun shale oil and its distillates was investigated (displayed in Fig. 10). In addition, the variation of heteroatomic compounds between Fushun shale oil and its liquid products derived from catalytic cracking process is shown in Figs. 11 and 12. It can be seen from Fig. 10 that the catalytic cracking conversion of each distillate gradually decreases as the distillation temperature increases. The LPG yield and gasoline yield gradually decrease, while the dry gas yield and coke

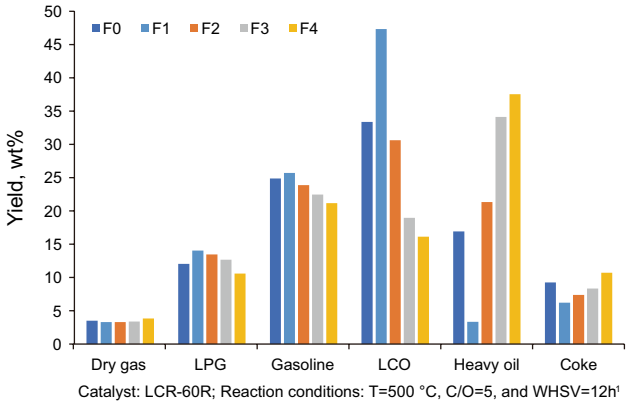

Fig. 10 Yields of various fractions from the catalytic cracking process. Please refer to Table 1 for the meaning of F0–F4

yield gradually increase. The one reason for these results is that, for each distillate, its density and CCR value gradually increase, while its hydrogen content and H/C ratio gradually decrease with the increase in distillation temperature (refer to Table 1). More importantly, as the boiling point of the fraction increases, the number and the molecular weight of heteroatomic compounds are increasing (refer to Figs. 1 and 5), especially for BNCs, including N1, N1O1, and N2, resulting in more poisoning to the catalyst and lower catalytic cracking conversion. Because the poisoning effect is not only related to the content of BNCs, but also to the structure and composition of BNCs (Li et al. 2011; Chen et al. 2017).

After catalytic cracking of Fushun shale oil, 43.89% of the nitrogen is distributed in the liquid product and 55.23% of the nitrogen converts into coke deposited on the catalyst. From Fig. 11, before and after catalytic cracking reaction, the classes of BNCs remain unchanged. Except for N2 species, the relative abundances of other BNCs all decrease. This shows that the basic N2 species are more difficult to convert into coke during the catalytic cracking process and the most of them still remain in the liquid products. Furthermore, the classes and relative abundances of NBHCs change significantly before and after the catalytic cracking reaction (Fig. 11b). The relative abundance of neutral N1 species in the liquid product is much higher than that in the feed of Fushun shale oil, while the relative abundances of other NBHCs reduced by different degrees and some even disappear in the liquid products, such as N1O2, O3, and O4. This is because the oxygen atoms in non-basic compounds are mostly in the form of carbonyl or carboxyl groups which are easy to be removed through decarboxylation or decarboxylation in catalytic cracking process (Chen et al. 2017). Interestingly, after catalytic cracking, the DBE values distribution of basic and neutral N1 species changes significantly (Fig. 12). The basic N1 species with the most abundant at DBE = 4, 5 and the neutral N1 species with the most abundant at DBE = 6, 9, and 12 in the feed of Fushun shale oil. However, in the liquid products, the relative abundances of basic N1 species with DBE > 5 obviously increase and the relative abundance of neutral N1 species mainly concentrated at DBE = 12. Our previous publication reported that the nitrogen compounds with DBE values smaller than 10 can easily diffuse into the micro-pores of the catalyst and preferentially adsorbed onto the acid sites (Chen et al. 2017). These nitrogen compounds can generally form coke deposited on the cracking catalysts through condensation and hydrogen transfer reactions, consequently resulting in decreasing of their relative abundance in the liquid products.

4 Conclusions

The distributions of molecular weight, type, class, and carbon number of heteroatomic compounds in Fushun shale oil distillates are identified by positive- and negative-ion ESI FT-ICR MS. There are nine classes of BNCs and eleven classes of NBHCs in the Fushun shale oil distillates, which

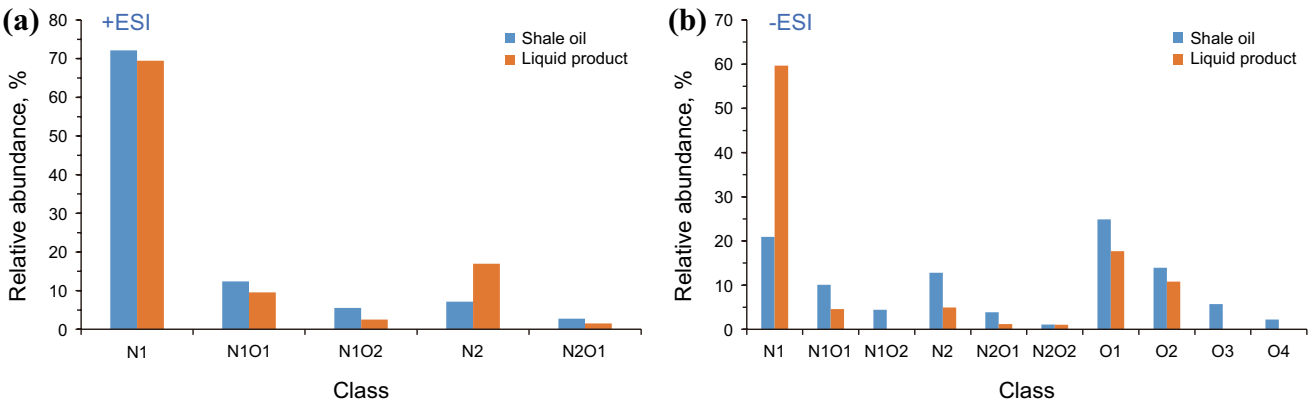

Fig. 11 Relative abundances (> 0.5%) of the heteroatomic classes in Fushun shale oil and its catalytic cracking liquid products

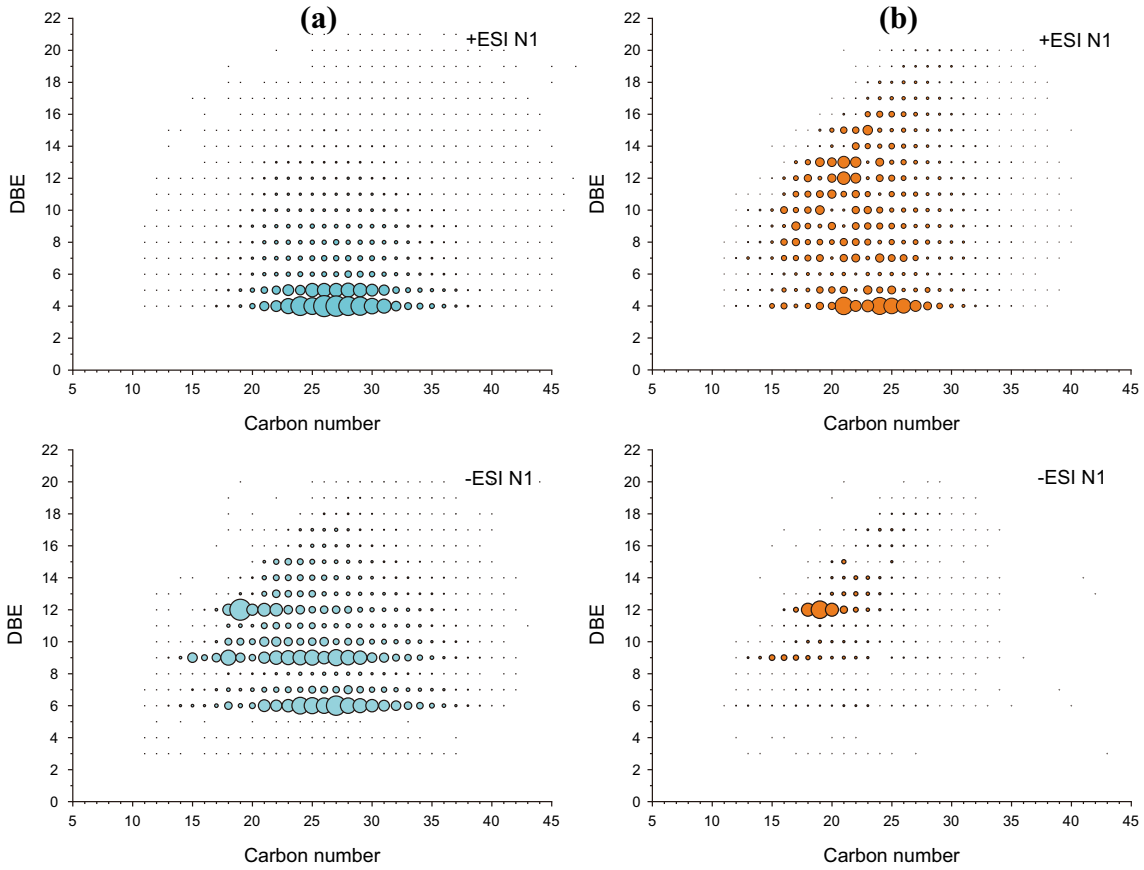

Fig. 12 Relative abundance plots of DBE versus carbon number of basic N1 and neutral N1 compounds in (**a**) Fushun shale oil and (**b**) its catalytic cracking liquid products. The area of a circle shows the relative abundance of each heteroatomic compound

are both more abundant than those in the parent shale oils and some conventional crude oils. The dominant BNCs in all the distillates are mainly basic N1 compounds, and their relative abundance gradually decreases with the increase in distillation temperature, while the relative abundance of multiheteroatomic BNCs gradually increases in heavier shale oil distillates. In the F1, F2, and F3 distillates, the dominant NBHCs are mainly acidic oxygen compounds, such as O2 and O1 compounds, while in the F4 fraction, neutral heteroatomic compounds, such as N1, N1O1, and N2 class species, become relatively abundant.

In each distillate, the dominant basic N1 compounds are pyridines and tetrahydroquinolines and they are separated into different distillates by alkylation (different C_n) but not by aromaticity (different DBE values). The other two basic N1O1 and N2 class species are separated into different distillates by both alkylation and aromaticity. The dominant acidic O1 and O2 compounds are phenols and aliphatic acids and they are separated into different distillates by alkylation but not by aromaticity. The neutral N1 and N2 compounds have similar distributions of DBE values and C_n in each distillate, and they are mainly separated into different distillates by aromaticity, with alkylation as a supplement. In addition, as the boiling point of the distillates increases, the catalytic cracking conversion of each distillate gradually decreases, mainly due to the increase in the number and molecular weight of its heteroatomic compounds, the increase in density and CCR value, as well as the decrease of hydrogen content and H/C ratio. After the catalytic cracking of Fushun shale oil, the classes of BNCs in the liquid products remain unchanged, while the classes and relative abundances of NBHCs vary significantly.

Acknowledgments This work was supported by the National Natural Science Foundation of China (21776312).

Compliance with ethical standards

Conflict of interest The authors declare no conflict of interest.

References

Akash BA. Characterization of shale oil as compared to crude oil and some refined petroleum products. Energy Sources. 2003;25:1171–82.

Bae EJ, Na J, Chung S, Kim H, Kim S. Identification of about 30000 chemical components in shale oils by electrospray ionization (ESI) and atmospheric pressure photoionization (APPI) coupled with 15 T Fourier transform ion cyclotron resonance mass spectrometry (FT-ICR MS) and a comparison to conventional oil. Energy Fuels. 2010;24:2563–9. https://doi.org/10.1021/ef100060b.

Chen XB, Li N, Yang YQ, Yang CH, Shan HH. Novel propylene production route: Utilizing hydrotreated shale oil as feedstock via two-stage riser catalytic cracking. Energy Fuels. 2015;29:7190–5. https://doi.org/10.1021/acs.energyfuels.5b02076.

Chen XB, Li T, Liu YB, Shan HH, Yang CH, Li CY. Characterization of nitrogen compounds in vacuum residue and their structure comparison with coker gas oil. China Pet Process Petrochem Technol. 2014;16:33–41.

Chen XB, Li T, Xin L, Yang YQ, Shan HH, Yang CH. Inductive effect of basic nitrogen compounds on coke formation during the catalytic cracking process. Catal Commun. 2016;74:95–8. https://doi.org/10.1016/j.catcom.2015.11.008.

Chen XB, Liu YB, Li SJ, Feng X, Shan HH, Yang CH. Structure and composition changes of nitrogen compounds during the catalytic cracking process and their deactivating effect on catalysts. Energy Fuels. 2017;31:3659–68. https://doi.org/10.1021/acs.energyfuels.6b03230.

Chen XB, Shen BX, Sun JP, Wang CX, Shan HH, Yang CH, Li CY. Characterization and comparison of nitrogen compounds in hydrotreated and untreated shale oil by electrospray ionization (ESI) Fourier transform ion cyclotron resonance mass spectrometry (FT-ICR MS). Energy Fuels. 2012;26:1707–14. https://doi.org/10.1021/ef201500r.

Chishti HM, Williams PT. Aromatic and hetero-aromatic compositonal changes during catalytic hydrotreatment of shale oil. Fuel. 1999;78:1805–15. https://doi.org/10.1016/S0016-2361(99)00089-7.

Cho Y, Jin J, Witt M, Birdwell JE, Na J, Roh N, Kim S. Comparing Laser desorption ionization and atmospheric pressure photoionization coupled to Fourier transfer ion cyclotron resonance mass spectrometry to characterize shale oils at the molecular level. Energy Fuels. 2013;27:1830–7. https://doi.org/10.1021/ef3015662.

Feng Y, Van Le DT, Pomerantz AE. The chemical composition of bitumen in pyrolyzed Green River oil shale: characterization by ^{13}C NMR spectroscopy. Energy Fuels. 2013;27:7314–23. https://doi.org/10.1021/ef4016685.

Fletcher TH, Gillis R, Adams J, Hall T. Characterization of macromolecular structure elements from a Green River oil shale, II. Characterization of pyrolysis products by ^{13}C NMR, GC/MS, and FT IR. Energy Fuels. 2014;28:2959–70. https://doi.org/10.1021/ef500095j.

Fu JM, Klein GC, Smith DF, Kim SW, Rodgers RP, Hendrickson CL, Marshall AG. Comprehensive compositional analysis of hydrotreated and untreated nitrogen-concentrated fractions from syn-crude oil by electron ionization, field desorption ionization and electrospray ionization ultrahigh-resolution FT-ICR mass spectrometry. Energy Fuels. 2006;20:1235–41. https://doi.org/10.1021/ef060012r.

Gao S, Han DY, Hou DD, Cao CY, Cao ZB. Utilization of phenolic compounds in light fraction of Fushun shale oil. Petrol Proc Prtrochem. 2019;50:53–7 **(In Chinese)**.

Guo SH, Qin KZ, Sun BI, Sun J. Nitro-containing compounds in the Chinese light shale oils. Oil Shale. 1993;10:165–77.

Han DY, Li GX, Cao ZB, Zhai XY, Yuan MM. A study on the denitrogenation of Fushun shale oil. Energy Sources Part A Recovery Util Environ Effects. 2013;35:622–8. https://doi.org/10.1080/15567036.2010.509085.

Hepbasli A. Oil shale as an alternative energy source. Energy Sources. 2004;26:107–18.

Hillier JL, Fletcher TH, Solum MS, Pugmire RJ. Characterization of macromolecular structure of pyrolysis products from a Colorado Green River oil shale. Ind Eng Chem Res. 2013;52:15522–32. https://doi.org/10.1021/ie402070s.

Hughey CA, Rodgers RP, Marshall AG. Resolution of 11 000 compositionally distinct components in a single electrospray ionization Fourier transform ion cyclotron resonance mass spectrum of crude oil. Anal Chem. 2002a;74:4145–9. https://doi.org/10.1021/ac020146b.

Hughey CA, Rodgers RP, Marshall AG, Qian KN, Robbins WK. Identification of acidic NSO compounds in crude oils of different geochemical origins by negative ion electrospray Fourier transform ion cyclotron resonance mass spectrometry. Org Geochem. 2002b;33:743–59. https://doi.org/10.1016/S0146-6380(02)00038-4.

Jin JM, Kim S, Birdwell JE. Molecular characterization and comparison of shale oils generated by different pyrolysis methods. Energy Fuels. 2012;26:1054–62. https://doi.org/10.1021/ef201517a.

Jones DM, Watson JS, Meredith W, Chen M, Bennett B. Determination of naphthenic acids in crude oils using nonaqueous ion exchange solid-phase extraction. Anal Chem. 2001;73:703–7. https://doi.org/10.1021/ac000621a.

Kelemen SR, Afeworki M, Gorbaty ML, Sansone M, Kwiatek PJ, Walters CC, Freund H, Siskin M. Direct characterization of kerogen by X-ray and solid-state ^{13}C nuclear magnetic resonance methods. Energy Fuels. 2007;21:1548–61. https://doi.org/10.1021/ef060321h.

Klein GC, Ansgtrom A, Rodgers RP, Marshall AG. Use of saturates/aromatics/resins/asphaultenes (SARA) fractionation to determine matrix effects in crude oil analysis by electrospray ionization Fourier transform ion cyclotron resonance mass spectrometry. Energy Fuels. 2006;20:668–72. https://doi.org/10.1021/ef050353p.

Korth J, Ellis J, Crisp PT, Hutton AC. Chemical characterization of shale oil from Duaringa, Australia. Fuel. 1988;67:1331–5. https://doi.org/10.1016/0016-2361(88)90113-5.

Li ZK, Wang G, Shi Q, Xu CM, Gao JS. Retardation effect of basic nitrogen compounds on hydrocarbons catalytic cracking in coker gas oil and their structural identification. Ind Eng Chem Res. 2011;50:4123–32. https://doi.org/10.1021/ie102117x.

Qian KN, Robbins WK, Hughey CA, Cooper HJ, Rodgers RP, Marshall AG. Resolution and identification of elemental compositions for more than 3000 crude acids in heavy petroleum by negative-ion microelectrospray high-field Fourier transform ion cyclotron resonance mass spectrometry. Energy Fuels. 2001a;15:1505–11. https://doi.org/10.1021/ef010111z.

Qian KN, Rodgers RP, Hendrickson CL, Emmett MR, Marshall AG. Reading chemical fine print: resolution and identification of 3000 nitrogen-containing aromatic compounds from a single electrospray ionization Fourier transform ion cyclotron resonance mass spectrum of heavy petroleum crude oil. Energy Fuels. 2001b;15:492–8. https://doi.org/10.1021/ef000255y.

Regtop RA, Crisp PT, Ellis J. Chemical characterization of shale oil from Rundle, Queensland. Fuel. 1982;61:185–92. https://doi.org/10.1016/0016-2361(82)90233-2.

Shi Q, Hou D, Chung KH, Xu CM, Zhao SQ, Zhang YH. Characterization of heteroatom compounds in a crude oil and its saturates, aromatics, resins, and asphaltenes (SARA) and non-basic nitrogen fractions analyzed by negative-ion electrospray ionization Fourier transform ion cyclotron resonance mass spectrometry. Energy Fuels. 2010a;24:2545–53. https://doi.org/10.1021/ef901564e.

Shi Q, Xu CM, Zhao SQ, Chung KH, Zhang YH, Gao W. Characterization of basic nitrogen species in coker gas oils by positive-ion electrospray ionization Fourier transform ion cyclotron resonance mass spectrometry. Energy Fuels. 2010b;24:563–9. https://doi.org/10.1021/ef9008983.

Shi Q, Zhao SQ, Xu ZM, Chung KH, Zhang YH, Xu CM. Distribution of acids and neutral nitrogen compounds in a Chinese crude oil and its fractions: characterized by negative-ion electrospray ionization Fourier transform ion cyclotron resonance mass spectrometry. Energy Fuels. 2010c;24:4005–11. https://doi.org/10.1021/ef1004557.

Shue FF, Yen TF. Concentration and selective identification of nitrogen- and oxygen-containing compounds in shale oil. Anal Chem. 1981;53:2081–4. https://doi.org/10.1021/ac00236a030.

Smith DF, Rahimi P, Teclemariam A, Rodgers RP, Marshall AG. Characterization of Athabasca bitumen heavy vacuum gas oil distillation cuts by negative/positive electrospray ionization and automated liquid injection field desorption ionization Fourier transform ion cyclotron resonance mass spectrometry. Energy Fuels. 2008;22:3118–25. https://doi.org/10.1021/ef8000357.

Snyder LR. Nitrogen and oxygen compound types in petroleum. Total analysis of an 850–1000°F distillate from a California crude oil. Anal Chem. 1969;41:1084–94. https://doi.org/10.1021/ac60277a008.

Solum MS, Mayne CL, Orendt AM, Pugmire RJ. Characterization of macromolecular structure elements from a Green River oil shale, I Extracts. Energy Fuels. 2014;28:453–65. https://doi.org/10.1021/ef401918u.

Stanford LA, Kim S, Rodgers RP, Marshall AG. Characterization of compositional changes in vacuum gas oil distillation cuts by electrospray ionization Fourier transform-ion cyclotron resonance (FT-ICR) mass spectrometry. Energy Fuels. 2006;20:1664–73. https://doi.org/10.1021/ef060104g.

Sun YH, Bai FT, Liu BC, Liu YM, Guo MY, Guo W, Wang QW, Lü XS, Yang F, Yang Y. Characterization of the oil shale products derived via topochemical reaction method. Fuel. 2014;115:338–46. https://doi.org/10.1016/j.fuel.2013.07.029.

Tong JH, Han XX, Wang S, Jiang XM. Evaluation of structural characteristics of Huadian oil shale kerogen using direct techniques (solid-state ^{13}C NMR, XPS, FT-IR, and XRD). Energy Fuels. 2011;25:4006–13. https://doi.org/10.1021/ef200738p.

Tong JH, Liu JG, Han XX, Wang S, Jiang XM. Characterization of nitrogen-containing species in Huadian shale oil by electrospray ionization Fourier transfer ion cyclotron resonance mass spectrometry. Fuel. 2013;104:365–71. https://doi.org/10.1016/j.fuel.2012.09.042.

Williams PT, Chishti HM. Reaction of nitrogen and sulphur compounds during catalytic hydrotreatment of shale oil. Fuel. 2001;80:957–63. https://doi.org/10.1016/S0016-2361(00)00189-7.

Xin L, Liu XX, Chen XB, Feng X, Liu YB, Yang CH. Efficient conversion of light cycle oil into high-octane-number gasoline and light olefins over a mesoporous ZSM-5 catalyst. Energy Fuels. 2017;31:6968–76. https://doi.org/10.1021/acs.energyfuels.7b00852.

Yu H, Li S, Jin G. Catalytic hydrotreating of the diesel distillate from Fushun shale oil for the production of clean fuel. Energy Fuels. 2010;24:4419–24. https://doi.org/10.1021/ef100531u.

Zhu XC, Shi Q, Zhang YH, Pan N, Xu CM, Chung KH, Zhao SQ. Characterization of nitrogen compounds in coker heavy gas oil and its subtractions by liquid chromatographic separation followed by Fourier transform ion cyclotron resonance mass spectrometry. Energy Fuels. 2011;25:281–7. https://doi.org/10.1021/ef101328n.